

### Tabulation of Binary Aluminides

The periodic chart of Table III presents the phases of the binary aluminum systems for 77 of the elements. For systems with small solubilities and no intermediate phases, a dash (–) is indicated. For the others, the crystal structure type of each  $\text{MAI}_x$  phase is listed with increasing  $x$  from top to bottom. When two or more structures are given for the same composition, the form stable at the highest temperature is listed first followed by the lower temperature phases. The structure type formulas are given with the Al position last, e.g.,  $\text{Ni}_3\text{Sn}$  for  $\text{La}_3\text{Al}$  and  $\text{SnNi}_3$  for  $\text{LaAl}_3$ . In a few instances, metastable phases of practical importance are listed in parentheses. Table IV tabulates each of the structure types cited, followed by its Pearson structure symbol<sup>14</sup> and a list of the binary aluminides with that structure. When the phase exists for a wide composition range, the range of values of  $x$  is indicated. The symbols  $\alpha$ -,  $\beta$ -,  $\gamma$ -, etc., are used for phases at various temperatures for the same composition. The lowest temperature phase is designated by  $\alpha$ -. When only one phase has been characterized for a given structure, it is followed by a large black dot (•). In some instances, some non-aluminide phases, particularly of Ga and In, but sometimes also B and Tl, are listed to illustrate the range of elements that can combine with the elements with  $s^2p$  atomic ground state configurations. In some instances, when the composition of the aluminide differed appreciably from the composition of the crystal type formula because of vacancies, the conventional crystal type was replaced by that of a phase with a composition close to that of the aluminide. Because of the complexity of the aluminide systems and the occurrence of high-temperature phases that often transform to metastable structures upon cooling, many of the systems are not completely characterized. *Pearson's Handbook*<sup>14</sup> lists many reported aluminide phases that were excluded from Table IV because

it is believed that they are metastable. In some instances, when it was not possible to make a clear decision, the formula is followed by a question mark. A great deal of additional work is needed to completely establish the stable phases at low pressures. Of course, additional structures are expected at higher pressures. At the far right hand side of Table IV, an attempt has been made to characterize the general types of structures that relate to the Hume-Rothery rules.<sup>10</sup> For example, if the coordination corresponds closely to that for the c12 bcc structure which should have 1–1.5  $s,p$  electrons per atom, the symbol I is used. For hcp structures, the symbol II is used, and for ccp structures, the symbol III is used. Structures related to the  $\beta$ -Mn structure are labeled  $\beta$ -Mn. Structures related to the  $\gamma$ -brass structures are labeled  $\gamma$ . These last two are part of a large group for which substantial size differences result in structures with high coordination numbers. The symbol F–K for the Frank–Kasper structures<sup>15,16</sup> is used for some of these structures. In addition to effects of size differences, the directional character of the bonding may cause distortions.

References are cited for each structure to provide additional information about the crystal structures and the phase diagrams. The systems without intermediate phases that are listed in Table III are not cited in Table IV. The references are as follows: Bi, Pb;<sup>17</sup> Ga, Na, Zn;<sup>18</sup> K, Rb;<sup>19</sup> Be;<sup>20</sup> Cd;<sup>21</sup> Cs;<sup>22</sup> Ge;<sup>23</sup> Hg;<sup>24</sup> In;<sup>18,25</sup> Si;<sup>26</sup> Sn;<sup>27</sup> Tl.<sup>28</sup>

**Acknowledgment.** I wish to acknowledge the contribution of challenging questions of my students and interactions with John Norman and George Reynolds of MSNW, Inc. This work was supported by the Director, Office of Energy Research, Office of Basic Energy Sciences, Materials Sciences Division of the United States Department of Energy under Contract No. DE-AC03-76SF00098.

## Catalytic Oxidation of Carbon Monoxide on Palladium. 1. Effect of Pressure

S. M. Landry, R. A. Dalla Betta, J. P. Lü, and M. Boudart\*

Department of Chemical Engineering, Stanford University, Stanford, California 94305  
(Received: November 6, 1989)

The turnover rate for CO oxidation on palladium increases by a factor of 7.4, at 445 K and an equimolar ratio of reactants, when the total pressure increases from  $10^{-6}$  to  $10^2$  mbar. This effect of pressure is contrary to that expected from previous kinetic studies that predict no effect of pressure on rate, with one exception. Additionally, the apparent activation energy changes from ca. 110  $\text{kJ mol}^{-1}$  at high pressure ( $10^2$  mbar) to ca. 75  $\text{kJ mol}^{-1}$  at lower pressures ( $10^{-1}$  and  $10^{-6}$  mbar), suggesting a change in reaction mechanism with pressure.

### Introduction

The catalytic oxidation of CO on palladium has been studied in the vicinity of 450 K, at low pressure (ca.  $10^{-6}$  mbar) on large single crystals<sup>1–3</sup> or model catalysts consisting of Pd particles (1–10 nm) supported on  $\alpha$ - $\text{Al}_2\text{O}_3$  single crystals,<sup>4–6</sup> and at high pressure (ca.  $10^2$  mbar) on Pd particles supported on porous  $\text{SiO}_2$  or  $\text{Al}_2\text{O}_3$ .<sup>7–9</sup> The reported rate, when measured, was proportional to the ratio of concentrations of  $\text{O}_2$  and CO, i.e., to  $[\text{O}_2]/[\text{CO}]$  except for one study<sup>9</sup> that reported the rate proportional to  $[\text{O}_2]^{0.9}/[\text{CO}]^{0.8}$ . In all cases, this suggests that the turnover rate  $v_t$  (i.e., the number of  $\text{CO}_2$  molecules converted per Pd surface atom per second) should not change at all, or only increase by a factor of less than 10, when total pressure increases by 8 orders of magnitude. Unfortunately, while values of  $v_t$  are available at

low pressure, this is not so at high pressure because the percentage metal exposed  $E$  was not reported in the latter case.

The purpose of the present work was to measure  $v_t$  at high pressure ( $10^2$  mbar) and at medium pressure ( $10^{-1}$  mbar) on a

(1) Ertl, G.; Koch, J. *Proceedings of the 5th International Congress on Catalysis*; Hightower, J., Ed.; North Holland: Amsterdam, 1973; paper No. 67.

(2) Engel, T.; Ertl, G. *J. Chem. Phys.* **1978**, *69*(3), 1267.

(3) Engel, T.; Ertl, G. *Adv. Catal.* **1979**, *28*, 1.

(4) Ladas, S.; Poppa, H.; Boudart, M. *Surf. Sci.* **1981**, *102*, 151.

(5) Ichikawa, S.; Poppa, H.; Boudart, M. *J. Catal.* **1985**, *91*, 1.

(6) Rumpf, F.; Boudart, M. *React. Kinet. Catal. Lett.* **1987**, *35*, 95.

(7) Tajbl, D. G.; Simmons, J. B.; Carberry, J. J. *Ind. Eng. Chem. Fundam.* **1966**, *5*, 171.

(8) Goldsmith, R. L. Ph.D. Dissertation, Massachusetts Institute of Technology, 1966.

(9) Cant, N. W.; Hicks, P. C.; Lennon, B. S. *J. Catal.* **1978**, *54*, 372.

\* Author to whom correspondence should be addressed.

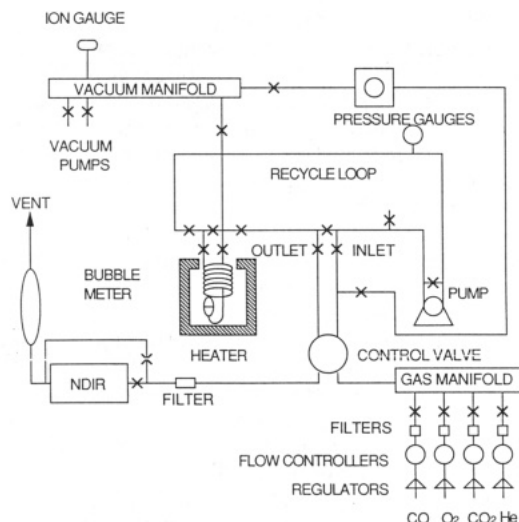


Figure 1. Continuous recycle reactor made of Pyrex and designed to operate as a continuously stirred tank reactor (CSTR).

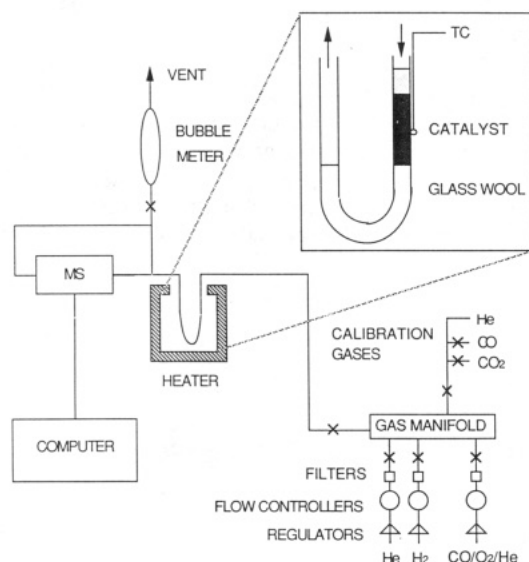


Figure 2. Integral flow reactor for medium pressure experiments consisting of a gas feed system, a packed catalyst bed in a Pyrex tube (inset), and a mass spectrometer.

supported Pd catalyst of known  $E$  to compare the results with  $v_t$  at low pressure ( $10^{-6}$  mbar).

### Experimental Section

**Catalysts.** The palladium on alumina catalyst (Engelhard Industries) contains 4.88 wt % Pd, based on dry catalyst as determined by atomic absorption, and percent metal exposed,  $E$ , was measured at 21% by CO and O<sub>2</sub> chemisorption as well as by H<sub>2</sub> titration of preadsorbed oxygen.<sup>10</sup> Crystallite size was estimated at 6 nm by X-ray diffraction in good agreement with the value (5.6 nm) calculated from  $E$  with the assumption of spherical particles.<sup>10</sup> The same catalyst was used at high and medium pressures and the above value of  $E$  was used in all determinations of  $v_t$ .

**High Pressure.** The high-pressure experiments ( $10^2$  mbar) were conducted in a continuous flow recycle reactor mimicking a CSTR (continuous stirred tank reactor) made of Pyrex (Figure 1). Typically the feed stream contained equimolar amounts of CO and O<sub>2</sub> of ca. 0.5 mol s<sup>-1</sup> per mole of Pd surface atoms (site contact frequency, scf). Both reactant gases constituted about 10% of the feed stream, the remainder being He diluent. The recycle ratio was ca. 28:1. Reaction temperature was maintained with a temperature controller (Gardman Corp.) and heater. Temperature

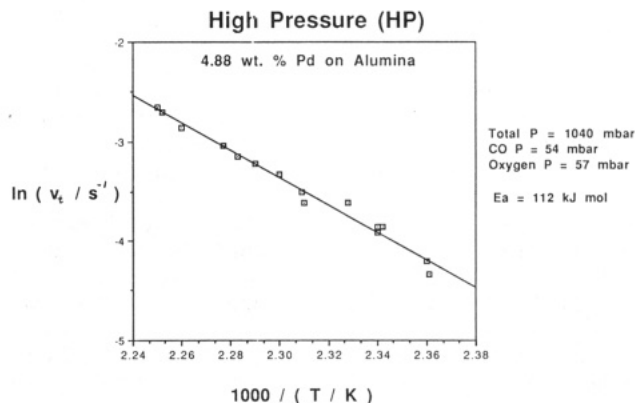


Figure 3. Turnover rate  $v_t$  for CO oxidation on 4.88 wt % Pd/Al<sub>2</sub>O<sub>3</sub> (21% metal exposed) at  $P_{O_2}/P_{CO} = 1.1$  and  $P_{TOT} \approx 1040$  mbar. Reactant gases were less than 10% of the total feed (balance was helium) and conversion was less than 0.5% per pass.

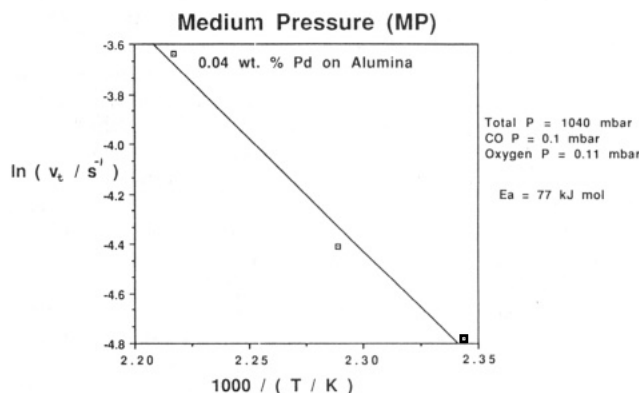


Figure 4. Turnover rate  $v_t$  for CO oxidation on 0.04 wt % Pd/Al<sub>2</sub>O<sub>3</sub> (21% metal exposed) at  $P_{O_2} = 1.1P_{CO} = 0.11$  mbar and  $P_{TOT} \approx 1040$  mbar with the balance helium. Conversion varied between 15 and 75%.

TABLE I: Experimental Values at  $v_t$  at High and Medium Pressure (This Work) and Low Pressure<sup>4</sup>

$P/\text{mbar}$	$10^{-6}$	$10^{-1}$	$10^2$
$v_t/\text{s}^{-1}$	0.010	0.024	0.074
relative $v_t$	1	2.4	7.4

of the catalyst bed was monitored by use of a glass jacketed Chromel–Alumel thermocouple in contact with the catalyst bed. Helium (99.995%) was purchased from Liquid Carbonic Corp. Reactant gases were obtained from Matheson Gas Products at 99.9% and 99.98% purity for CO and O<sub>2</sub>, respectively. In early experiments the composition of the inlet and outlet streams was measured with a Gow-Mac thermal conductivity detector, and the thermal conductivity difference was used to determine conversion. For later experiments the concentration of CO<sub>2</sub> in the outlet gas was monitored with a nondispersive infrared analyzer (Beckman Instruments Corp., Model 880).

In a typical experiment 100–200 mg of 100–400 mesh catalyst was used. Prior to each run, the catalyst was reduced at 573 K for 2 h in flowing H<sub>2</sub> (6 s<sup>-1</sup> scf, purified through a Pd thimble).

A typical run was conducted as follows: after reduction the system was evacuated and filled with reactant/diluent gases. The recycle pump was started and the inlet and outlet gases were allowed to equilibrate. The temperature was slowly ramped to reaction conditions (420–450 K). Total pressure was 1029–1040 mbar. Once a steady state was achieved and maintained for 1 h, rate data were taken. Total conversion varied between 2 and 12% with conversion per pass always less than 0.5%. No deactivation of the catalysts could be observed between the time steady state was achieved and termination of the longest run (72 h). Calculations<sup>11</sup> show the Thiele modulus to be less than  $10^{-4}$  (no pore diffusional limitations) and a maximum temperature dif-

(10) Benson, J. E.; Hwang, H. S.; Boudart, M. *J. Catal.* **1973**, *30*, 146.

(11) Landry, S. M. Ph.D. Dissertation, Stanford University, 1989.

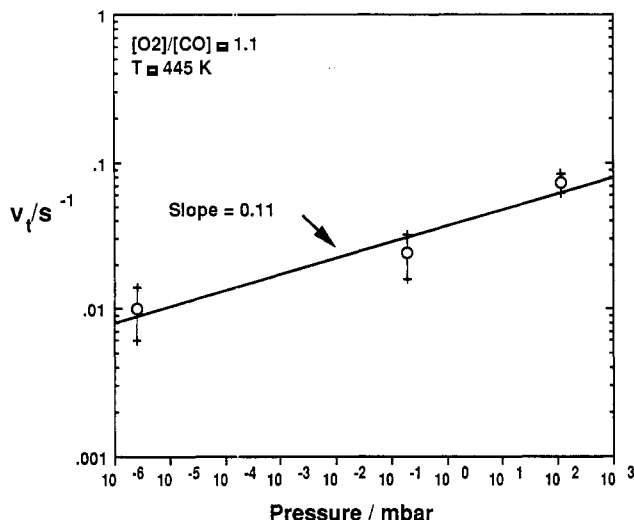


**Figure 5.** Effect of pressure on the turnover rate  $v_t$  of the oxidation of CO on Pd/alumina. The solid line is a least-squares logarithmic fit through the data. The point at  $10^{-6}$  mbar is from ref 4. The other points are from this work and have been adjusted to standard conditions ( $T = 445$  K and  $[O_2]/[CO] = 1.1$ ).

ference of 1.5 K between the catalyst surface and the gas phase (no external heat transfer limitations). Turnover rates were calculated by multiplying the CO molar feed rate by the measured conversion and dividing by the molar amount of Pd surface atoms in the reactor.

**Medium Pressure.** The medium-pressure experiments ( $10^{-1}$  mbar) were conducted in an integral flow reactor made of Pyrex (Figure 2). Reactant and diluent gases were mixed in a single gas cylinder (Matheson Gas Products) with 100 ppm CO, 100 ppm  $O_2$ , and He as the balance. The CO and  $O_2$  scf were ca.  $0.04$   $s^{-1}$  each. Reaction temperature was maintained with a programmable temperature controller (Omega Corp.) and heater. Temperature of the catalyst bed was monitored by use of a Chromel–Alumel thermocouple attached to the outer wall of the reactor. Separate experiments indicated a temperature difference of less than 0.1 K between the indicated value and that measured within the catalyst bed. The composition of the outlet stream was measured with a Hewlett-Packard 5970 mass spectrometer.

The catalyst was diluted 119:1 in calcined alumina powder (Alcoa Chemicals) to increase the bed diameter and facilitate accurate weighing. The accuracy of the dilution was checked by both dioxygen uptake comparison and inductively coupled plasma analysis for Pd content. In a typical experiment ca. 60 mg of 200–400 mesh diluted catalyst was used. Prior to each run, the catalysts were reduced at 573 K for 2 h in flowing  $H_2$  ( $136$   $s^{-1}$  scf) purified by passing the gas through a liquid nitrogen cooled zeolite trap.

A typical run was conducted as follows: After reduction the feed stream was switched from  $H_2$  to the  $CO/O_2/He$  mixture. After the outlet stream reached steady state, a calibration pulse of  $CO_2$  was injected. Once the system returned to steady state the temperature was ramped to reaction conditions (420–450 K) and maintained there for not less than 1 h. The heater was then removed and the system allowed to settle back to the original steady state at which time a second  $CO_2$  calibration pulse was injected. The experiment was terminated when the system returned to steady state. Total pressure was atmospheric. Conversion varied between 15 and 75% and was determined by comparing the CO and  $CO_2$  outlet concentrations at reaction conditions to the inlet CO concentration and the  $CO_2$  pulse peak area, respectively. Integral analysis (see Appendix) yielded an experimental rate constant which was then used to calculate a turnover rate at the inlet conditions. No deactivation of the catalysts could be observed. Calculations<sup>11</sup> show the Thiele modulus to be less than  $10^{-5}$  (no pore diffusional limitations) and a maximum temperature difference of 0.1 K between the catalyst surface and the gas phase (no external heat transfer limitations).

## Results

The high-pressure results are shown in Figure 3. The activation energy was determined to be  $112$   $kJ\ mol^{-1}$ . The medium-pressure results are shown in Figure 4. The activation energy was determined to be  $77$   $kJ\ mol^{-1}$ . We do not believe that the lower apparent activation energy found at medium pressure is a result of pore diffusional limitations for two reasons: first, our estimate<sup>11</sup> of the Thiele modulus indicates very clearly no such limitation, and second, a value of  $73$   $kJ\ mol^{-1}$  for the apparent activation energy can be calculated from the data of Ladas et al.<sup>4</sup> obtained at low pressures on model systems consisting of 6-nm Pd particles supported on a nonporous single-crystal  $\alpha-Al_2O_3$  support.

To determine the effect of pressure on turnover rate, we compare the results at a set of standard conditions (Table I). At 445 K our value of  $v_t$  for  $[O_2]/[CO] = 1.1$  at a total reactant pressure of  $1.1 \times 10^2$  mbar is  $0.074$   $s^{-1}$  and at  $6.4 \times 10^{-1}$  mbar and the same  $[O_2]/[CO]$  ratio the value is  $0.024$   $s^{-1}$ . Here and elsewhere,  $[M]$  denotes the number density of species  $M$  per  $cm^3$  or  $cm^2$  as the case may be. This compares to the value of  $0.01$   $s^{-1}$  measured by Ladas et al.<sup>4</sup> for the same  $[O_2]/[CO]$  ratio as 445 K at a total pressure of  $2.5 \times 10^{-6}$  mbar over the model catalyst just mentioned above. These are the main results of this work: the value of  $v_t$  is  $\sim 7$  times larger at high pressure than at low pressure for a pressure ratio of  $4.5 \times 10^7$  and  $\sim 2.5$  times higher at mid-range pressure than at low pressure for a pressure ratio of  $2.6 \times 10^5$  (Figure 5), and there is a large change in apparent activation energy between high and medium pressure.

## Discussion and Conclusion

Two sets of facts demand explanation. First, values of  $v_t$  at medium pressure and high pressure, as reported here, and values of  $v_t$  at low pressure as previously reported<sup>4</sup> show an increase in  $v_t$  with pressure. Over a change in pressure of 8 orders of magnitude  $v_t$  increases by a factor of  $\sim 7$ . This observation is incompatible with the rate expression  $v \propto [O_2]/[CO]$  reported in ref 4–8 as this rate expression predicts no change of  $v_t$  with pressure. But it is compatible with the rate expression of ref 9, namely  $v \propto [O_2]^{0.9}/[CO]^{0.8}$ . Yet the latter is probably indistinguishable from the former over a restricted range of pressure or reactant ratio. Besides it requires a mechanistic explanation that has not been provided. By contrast, the classical rate expression  $v \propto [O_2]/[CO]$  first found for CO oxidation on Pd at low pressure<sup>1</sup> can be explained easily on the basis of a Langmuir surface, as done by Langmuir himself on Pt<sup>12</sup> but it cannot account for the effect reported in this work.

The second fact to be explained is the large change in apparent activation energy  $E_{app}$  from low and medium pressure to high pressure, as first reported in this work. This suggests a change in mechanism as pressure goes up.

In conclusion both effects of pressure on  $v_t$  and  $E_{app}$  are large and well beyond experimental error. These effects are experimental fact. Their explanation may be subject to changes as a result of further work. For this reason, we prefer to present in a companion paper<sup>13</sup> our present interpretation of the facts as they now stand.

**Acknowledgment.** This work was supported in part by a continuing National Science Foundation (NSF) grant, currently NSF CBT 85-21375. S.M.L. acknowledges personal support from the U.S. Department of Defense. Some of the equipment used in this work was loaned by Catalytica Inc.

## Appendix

Conversion of the medium pressure ( $10^{-1}$  mbar) results to turnover rates was done as follows: Analysis of the experimental data points from the mass spectrometer gives only total conversion

(12) Langmuir, I. *Trans. Faraday Soc.* **1922**, *17*, 621.

(13) Landry, S. M.; Boudart, M. *J. Phys. Chem.*, to be submitted for publication.

of CO to CO<sub>2</sub>. Since the conversion is high (25–75%) the reactor must be treated as an integral reactor. For such a reactor

$$\frac{W}{F_{A0}} = \int_0^{x_A} \frac{dx_A}{-r_A} \quad (1)$$

where  $W$  is the weight of the catalyst,  $F_{A0}$  is the molar feed rate of component A,  $-r_A$  is the rate of disappearance of A, and  $x_A$  is the conversion of A. For the case of CO oxidation the rate is

$$-r_A = k \frac{[O_2]}{[CO]^\alpha} \quad (2)$$

At any value of conversion

$$[CO] = \frac{[CO]_0(1 - x_{CO})}{(1 + \epsilon_{CO}x_{CO})} \quad (3)$$

where  $[CO]_0$  is the inlet value of  $[CO]$ . The factor  $\epsilon_{CO}$  accounts for any volume change of the gas phase during the experiment. In our experiment  $\epsilon_{CO}$  has a value of  $1.50 \times 10^{-4}$  and the term  $\epsilon_{CO}x_{CO}$  is therefore neglected as compared to 1. This gives

$$[CO]^\alpha = ([CO]_0(1 - x_{CO}))^\alpha \quad (4)$$

and

$$[O_2] = [O_2]_0(1 - \frac{1}{2}x_{CO}) \quad (5)$$

Substitution of eq 4 and 5 into 2 yields

$$-r_A = k \frac{[O_2]_0(1 - \frac{1}{2}x_{CO})}{([CO]_0(1 - x_{CO}))^\alpha} \quad (6)$$

Substitution back into eq 1 yields an integral equation which we then solve for the experimental rate constant  $k_e$  in units of  $\text{cm}^3 \text{s}^{-1}$

$$k_e = \frac{F_{CO}^0}{W} \frac{[CO]^\alpha}{[O_2]} \frac{M_{Pd}}{E} \int_0^{x_{CO}} \frac{(1 - x_{CO})^\alpha}{(1 - \frac{1}{2}x_{CO})} dx_{CO} \quad (7)$$

where  $M_{Pd}$  is the molecular weight of Pd and  $E$  is the percentage metal exposed. Equation 7 can be evaluated analytically if  $\alpha = 1$  but must be evaluated numerically if  $\alpha \neq 1$ . For this purpose a simple program was run on a Hewlett-Packard 15C calculator. The accuracy of the numerical integration was checked by comparison to the analytical result with  $\alpha = 1$ . For each data point eq 7 was evaluated for three values of  $\alpha$ : 1.0, 0.9, and 0.884. In all cases the data fit a straight line equally well and yielded an activation energy of  $77 \text{ kJ mol}^{-1}$ . A turnover rate was then calculated at the inlet conditions as using

$$v_t = \frac{k[O_2]_0}{[CO]_0^\alpha} \quad (8)$$

where the same value of  $\alpha$  is used in eqs 7 and 8. As expected the value of  $v_t$  did not change significantly for any of the values of  $\alpha$  used.

**Registry No.** CO, 630-08-0; Pd, 7440-05-3.